Progress In Electromagnetics Research, PIER 29, 1–23, 2000

CLUTTER REDUCTION FOR SYNTHETIC APERTURE RADAR IMAGERY BASED ON ADAPTIVE WAVELET PACKET TRANSFORM

H. Deng and H. Ling

Department of Electrical and Computer Engineering
The University of Texas at Austin
Austin, TX 78712–1084, USA

Abstract–An adaptive wavelet packet transform (AWPT) algorithm is proposed to process synthetic aperture radar (SAR) imagery and remove background clutters from target images. Since target features are more efficiently represented using the wavelet packet bases, higher signal-to-clutter ratios (SCR) can be achieved in the wavelet transform domain. Consequently, clutters can be more effectively separated from the desired target features in the transform domain than in the original SAR domain. The processed results based on the MSTAR data set demonstrate the effectiveness of this algorithm for SAR clutter reduction.

1. INTRODUCTION

Synthetic aperture radar (SAR) images of ground targets after the focusing process generally consist of target images and clutters from background scattering [1]. The clutter signal is undesirable since it interferes with the actual target features in automatic target recognition (ATR) applications, and has to be removed before ATR processing. The traditional way to suppress clutter is to choose a threshold using CFAR that is based on the standard deviation and mean value of the clutter, and the threshold is applied to the SAR image chip to remove the clutter directly [2, 3]. However, this approach assumes that the target signal-to-clutter ratio (SCR) is large enough. If this assumption is not true, this approach results in either target feature loss or large clutter residues. In this work, we investigate the use of orthogonal basis transformation to increase the SCR for more effective clutter removal. More specifically, our approach is to find the best wavelet packet basis to represent a SAR image using the adaptive wavelet packet transform (AWPT) [4–9].

Wavelet packet basis is a generalization of the conventional wavelet basis. It retains the multi-resolution property of the conventional wavelet basis while abandoning the rigid constant-Q structure in the decomposition. Wavelet packets have been applied to image compression [7] and moment matrix sparsification [9] with good success. Theoretically they include regular pulse basis, FFT basis, short-time Fourier transform (STFT) basis, as well as conventional wavelet basis. In this application, we transform the SAR image into the wavelet packet basis to maximize the signal-clutter-ratio in the transform domain. Since a typical target image usually consists of point scatterers and more diffused region features, the multi-scaled wavelet basis is well suited to focus the target image. Clutter in the images, on the other hand, is statistically uncorrelated (or weakly correlated) from pixel to pixel, and the transformed clutter image under the same set of bases remains unfocused [8, 10, 11]. Therefore, we expect that the SCR can be increased by transforming the original image with an appropriately chosen set of wavelet packet basis. To determine the best basis for a SAR image, we implement the AWPT algorithm to search for the best wavelet packet

basis based on a cost function that describes how well the target signal is focused in the transform domain. Because clutter in a SAR image is usually not strictly white, we apply a frequency-dependent threshold to the transformed image. We then inverse-transform the thresheld image in the wavelet packet basis domain back to the SAR domain to obtain a de-cluttered target image.

This paper is organized as follows. In Section 2, we introduce the basic concept of wavelet packet basis. In Section 3, we discuss problem formulation and the algorithm for SAR clutter rejection based on the adaptive wavelet packet transform. In Section 4, we present the test results of the algorithm using the MSTAR data set [12]. In Section 5, we draw some conclusions from this work.

2. WAVELET PACKET BASIS FOR SIGNAL REPRESENTATION

A wavelet packet basis function can be expressed in the space domain as:

$$\varphi_{j,k}^{n}(x) = 2^{-j/2}\psi_n(2^{-j}x - k),\ k \in Z,\ j \in Z,\ n \in Z_+ \tag{1}$$

where k, j, and n denote the space shift, scale, and modulation index, respectively. The function ψ_n can be generated from the decompositions of both the scaling function and mother wavelet function using the "two-scale equation" [4, 5]. The parameter choice of a wavelet packet basis is not unique for a complete and orthogonal decomposition of a signal in L^2 space. For a wavelet packet basis function $\varphi_{j,k}^{n}$, we define its dyadic interval $I_{j,n} \subset \Re$ in the frequency domain as [4, 9]:

$$I_{j,n} = \left[2^{-j}n,\ 2^{-j}(n+1)\right) \tag{2}$$

For the complete and orthogonal wavelet basis functions $\{\varphi_j^n\}$ chosen to represent a signal in L^2 space, their dyadic intervals should be disjoint and cover the entire signal bandwidth, i.e.,

$$\bigcap_{j,n} I_{j,n} = [\emptyset] \tag{3}$$

and

$$\bigcup_{j,n} I_{j,n} = [0, 1) \tag{4}$$

Therefore, the wavelet packet basis function φ_j^n can be interpreted as a modulated wavelet with a central frequency of $2^{-j}(n+1/2)$ and a normalized bandwidth of 2^{-j}.

For two-dimension image decomposition, the 2-D wavelet packet basis function can be configured from two 1-D wavelet packet basis functions as follows:

$$U_{p,q}^j(m,n) = \psi_{j,m}^p \psi_{j,n}^q \tag{5}$$

In (5), we restrict the scales of the two 1-D basis functions to be the same. This guarantees the basis functions will be of the same size in the horizontal and vertical directions, and remove the inter-scale coupling terms in the transformed image. For a complete and orthogonal decomposition, the two 1-D basis functions in (5) must also meet the requirements in (3) and (4).

Assuming that the original image in the spatial (SAR) domain is $\{s(m,n),\ 0 \le m,\ n < N\}$, we define a set of complete and orthonormal 2-D wavelet packet basis functions:

$$\{U_{p,q}^j(k,l)\ 0 \le j < J,\ 0 \le p,\ q < 2^j,\ 0 \le k,\ l < N2^{-j}\} \tag{6}$$

where j denotes the scale, $J = \log_2(N)$, p and q are the frequency modulation indices, and k, l are the position indices. The decomposition coefficients of the image $s(m,n)$ using the wavelet packet basis (6) are:

$$\widetilde{S}_{p,q}^j(k,l) = \sum_m \sum_n s(m,n) U_{p,q}^j(k - 2^j m, l - 2^j n) \tag{7}$$

With the image extended to be periodic in the spatial domain, the total number of coefficients is exactly N^2 through the transform in (7). For convenience, we refer to the coefficients as simply a matrix $\{\widetilde{S}(m,n),\ 1 \le m,\ n \le N\}$ without explicit indication of j, p and q.

Given a SAR image $s(m,n)$, we set out to find the best wavelet packet basis to maximize the SCR in transform domain. In the other words, we try to make the transformed coefficient matrix $\{\widetilde{S}(m,n),\ 1 \le m,\ n \le N\}$ as sparse as possible.

3. SAR IMAGE CLUTTER REDUCTION USING ADAPTIVE WAVELET PACKET TRANSFORM

3.1 Statistical Signal Model

We assume that a focused SAR image in spatial domain is:

$$\{s(m,n),\ 0 \le m,\ n < N\} \tag{8}$$

Ignoring additive noise and possible multiplicative speckle noise in the image, we consider a SAR image that consists of only the target image and clutters generated from the background scattering [15]. Basically the target image and the clutters are non-overlapping in a SAR image, therefore there is:

$$s(m,n) = \begin{cases} t(m,n), & (m,n) \text{ in target area} \\ c(m,n), & (m,n) \text{ in clutter area} \end{cases} \quad 0 \le m,\ n < N \tag{9}$$

For a clutter pixel $c(m,n)$, it includes reflections from minute scatters inside this resolution cell. For modern coherent imaging radar with a quadrature receiver, it can be represented as:

$$\begin{aligned} c(m,n) &= \sum_{k=1}^{K} a_k \exp(j2\pi f_c \tau_k) \\ &= c_r + jc_i \end{aligned} \tag{10}$$

where a_k and τ_k are the magnitude and relative two-way propagation delay of the reflection from the k-th scatter in this clutter resolution cell. If we assume those variables are statistically independent and K is large, according to Central limit theorem the sum in (10) tends to be a complex Gaussian random variable, and its amplitude is approximately Rayleigh distributed [13, 16, 17]. Although, for high-resolution radar with a low gazing angle, the amplitude is closer to be Weibull distributed for ground clutters, Rayleigh approximation is accurate enough, especially for the distribution near the mean [15].

Another important assumption about SAR clutters is that clutters in different pixels are statistically independent [13–16]. Therefore, we have:

$$E\left[c(m,n)c^*(p,q)\right] = \sigma_c^2 \delta(p-m)\delta(q-n) \tag{11}$$

where σ_c is the clutter standard deviation, and δ is the Dirac function.

Using ergodic characteristics of independent identical random variables, the statistical mean value in (11) can be approximated with a spatial average:

$$\begin{aligned} E\left[c(m,n)c^*(p,q)\right] &\cong \sum_k \sum_l c(k,l)c^*(k+p-m, l+q-n) \\ &\cong \sigma_c^2 \delta(p-m)\delta(q-n) \end{aligned} \tag{12}$$

From (12) we find the clutters are spatially uncorrelated, which provide clutters a distinct feature from the target signal. But we must note that for SAR clutters there is some weak correlation among adjacent pixels, thus (12) is not quite right if $p-m$ and $q-n$ are close to zeros.

Generally the target area is in the central part of a SAR image, and the clutters are located in surrounding parts. We define that the target signal is zero in clutter area, and the clutter is zero in target area, i.e.,

$$t(m,n) = 0, \quad (m,n) \text{ in clutter area} \tag{13}$$

$$c(m,n) = 0, \quad (m,n) \text{ in target area} \tag{14}$$

Because zero values don't contribute anything to the summation in (12), the definition in (14) doesn't affect the autocorrelation property of clutters in (12) as long as there are enough actual clutter samples in the correlation. Also the zeros in (13) won't affect the autocorrelation property of target image.

Considering (9), (13), and (14), we have:

$$s(m,n) = t(m,n) + c(m,n) \quad 0 \le m,\ n < N \tag{15}$$

With the additive model in (15) for a SAR image, we need to find the best wavelet packet basis to maximize Signal-to-Clutter ratio in the transform domain.

3.2 Best Wavelet Packet Basis for Maximization of Signal-to-Clutter Ratio

If we apply a wavelet packet basis shown in (6) to a SAR image $s(m,n)$ in (15), the transform coefficients are:

$$\begin{aligned} \widetilde{S}_{p,q}^j(k,l) &= \sum_m \sum_n s(m,n) U_{p,q}^j(k-2^j m, l-2^j n) \\ &= \widetilde{T}_{p,q}^j(k,l) + \widetilde{C}_{p,q}^j(k,l) \end{aligned} \tag{16}$$

where:

$$\widetilde{T}^j_{p,q}(k,l) = \sum_m \sum_n t(m,n) U^j_{p,q}(k - 2^j m, l - 2^j n) \tag{17}$$

$$\widetilde{C}^j_{p,q}(k,l) = \sum_m \sum_n c(m,n) U^j_{p,q}(k - 2^j m, l - 2^j n) \tag{18}$$

are the coefficients for target image and clutters, respectively.

Because a liner combination of independent Gaussian random variable, the clutter coefficients still are Gaussian distributed. If we rewrite (18) into a simple form, and note that wavelet packet basis is orthonormal, there are:

$$\widetilde{C}(k,l) = \sum_m \sum_n c(m,n) U(k,l,m,n) \tag{19}$$

and

$$\begin{aligned}
&E\left[\widetilde{C}(k,l)\widetilde{C}^*(i,j)\right] \\
&= E\left[\sum_m \sum_n c(m,n) U(k,l,m,n) \sum_p \sum_q c^*(p,q) U(i,j,p,q)\right] \\
&= \sum_m \sum_n \sum_p \sum_q E\left[c(m,n)c^*(p,q)\right] U(k,l,m,n) U(i,j,p,q) \\
&= \sum_m \sum_n \sum_p \sum_q \sigma_c \delta(p-m)\delta(q-n) U(k,l,m,n) U(i,j,p,q) \\
&= \sum_m \sum_n \sigma_c U(k,l,m,n) U(i,j,m,n) \\
&= \sigma_c \delta(i-k)\delta(j-l)
\end{aligned} \tag{20}$$

Therefore, the clutter coefficients are uncorrelated, thus independent Gaussian statistical variables with the same mean and variance as those of the clutter in spatial domain.

We have demonstrated that the statistical characteristics of SAR image clutters don't change after wavelet packet basis transformation. But target image is correlated to itself. We need to find a wavelet packet basis to make transformed target image further concentrated, and increase the signal-to-clutter ratio in transform domain, in other words, we need to make transformed target image sparse. A cost functions is needed to measure the sparsity of the transformed signal, thus

the best wavelet packet basis can be found for a specific image to achieve the maximum sparsity in the transformed image. A typical cost function for sparsity is entropy function. But entropy function itself is not an additive cost function, which makes it inapplicable in a fast global best basis search algorithm. A modified additive entropy function was proposed [18, 19], but it requires computation-intensive logarithm operation to evaluate function cost, and is unstable in the environment with clutter or noise interference. Alternatively we use l^p energy concentration function as cost function in this application. The l^p energy concentration function of a data sequence $\{x(k),\ k = 1, 2, \ldots, K\}$ is defined as:

$$C = \sum_{k=1}^{K} |x(k)|^p \qquad 0 < p < 2 \tag{21}$$

For a transformed SAR image with a coefficient matrix $\left[\widetilde{S}\right]$, the cost function is:

$$C = \sum_{k} \sum_{l} \left|\widetilde{S}(k,l)\right|^p \qquad 0 < p < 2 \tag{22}$$

For convenience and efficiency, we usually choose: $p = 1$ in (22). Supposing we transform a sequence $\{x_1, x_2, \cdots, x_L\}$ into another sequence $\{\tilde{x}_1, \tilde{x}_2, \cdots, \tilde{x}_L\}$ with a wavelet packet basis using the cost function of (22), the transformed sequence is the sparsest if all of them excerpt one are zeros, accordingly the cost is the minimum in this case. We illustrate the best basis selection criterion based on the energy concentration cost function in (21) using a simple case: assuming that a data sequence is $\{x_1, x_2\}$ with energy equal to 1, and its orthonormal basis transform coefficients are $\{\tilde{x}_1, \tilde{x}_2\}$, we have:

$$|\tilde{x}_1|^2 + |\tilde{x}_2|^2 = 1 \tag{23}$$

The cost function is:

$$Cost = |\tilde{x}_1| + |\tilde{x}_2| \tag{24}$$

As shown in Figure 1, transformed data must be a point on the circle with radius of 1 because of constant energy constraint. The Lines a, b, and c are the energy concentration cost functions with $p = 1$. The cost function lines must cross the one-fourth of the circle to satisfy

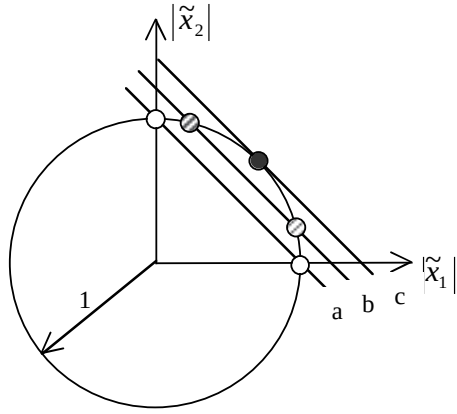

Figure 1. Relationship between the sparsity of a basis transformed signal and the energy concentration cost function.

the energy constraint. Apparently on Line c the blank point is the transformed data, but it has the highest cost, and worst sparsity. On Line a, two white points are the possible transformed data. They have the lowest cost, and best sparsity for all possible basis transformation. The gray points on Line b are the transformed data with cost and sparisty between the best and the worst. Therefore, based on the energy concentration cost function, we can effectively find the best transform basis to maximize the sparsity of the transformed signals.

Due to the non-overlapping of target and clutter in spatial domain, mostly the coefficients for target and clutter are also separated in the finer scales in the transform domain. Thus the total cost of the transformed SAR images in (16) is approximately equal to the sum of the costs of transformed target images and clutters, i.e.,

$$Cost\left(\left[\widetilde{\mathbf{S}}\right]\right) \cong Cost\left(\left[\widetilde{\mathbf{T}}\right]\right) + Cost\left(\left[\widetilde{\mathbf{C}}\right]\right) \tag{25}$$

where $\left[\widetilde{\mathbf{S}}\right]$, $\left[\widetilde{\mathbf{T}}\right]$, and $\left[\widetilde{\mathbf{C}}\right]$ are the transform coefficient matrices for the whole SAR image, target image, and clutters, respectively. The cost of transformed clutters doesn't change because they are the random variables with exactly the same distribution as that of the original clutters in spatial domain. The minimization of the cost of the whole transformed SAR image is equivalent to the minimization of that of the transformed target image, and thus the maximization of target signal-to-clutter ratio in the transform domain.

3.3 Implementation of Adaptive Wavelet Packet Transform for SAR Images

Theoretically we can apply every possible wavelet packet basis to a SAR image, evaluate the cost of the every transformed image, and find the best wavelet packet basis with the least cost. But the brutal force computation is impractical to implement because there are too many eligible wavelet packet bases for a specific application and the direct convolution in (7) is computationally too costly. Fortunately, in [18] a fast decomposition algorithm was proposed to search the best wavelet packet for a data sequence based on additive cost function, and it can be readily adapted to 2-D SAR image processing.

Generally the original SAR image is the discretized samples using pulse basis, and it can be approximated as the coefficients of wavelet packet basis with the highest spatial resolution, i.e., in the finest scale. The decomposition coefficients in the next scale are related to the ones in current scale by "2-scale equations" using a pair of quadrature filters $\{h(n)\}$ and $\{g(n)\}$.

Assuming that the initial image samples are represented with a matrix $[\mathbf{S}]$, its decomposition coefficients at the next scale can be obtained through the convolution and down-sampling of $[\mathbf{S}]$ and quadrature filter impulse responses $\{h(n)\}$ and $\{g(n)\}$, i.e.,

$$\begin{aligned} S^{(2)}_{HH}(m,n) &= \sum_k \sum_l s(k,l)g(2m-k)g(2n-l) \\ S^{(2)}_{LH}(m,n) &= \sum_k \sum_l s(k,l)h(2m-k)g(2n-l) \\ S^{(2)}_{HL}(m,n) &= \sum_k \sum_l s(k,l)g(2m-k)h(2n-l) \\ S^{(2)}_{LL}(m,n) &= \sum_k \sum_l s(k,l)h(2m-k)h(2n-l) \end{aligned} \tag{26}$$

where $\{h(n)\}$ and $\{g(n)\}$ denote the impulse responses of low- and high-pass Quadrature Filters (QFs), respectively. The decomposition in (26) is widely referred as quadtree decomposition, which is illustrated in Figure 2. The quadtree decompositions can be applied recursively until the coarsest scale is reached. Apparently the decomposition at each scale needs $O(\mathrm{N}^2)$ operations, and the number of total available scales is about $\log_2(\mathrm{N})$. Therefore, the total computation cost to implement the full decomposition from spatial domain to frequency

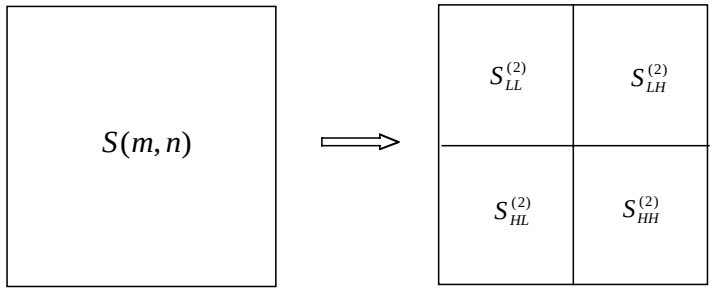

Figure 2. Quadtree decomposition structure.

domain is about $O(\mathrm{N}^2\log_2 N)$ operations using the quadtree decomposition method. Because the cost function is additive, the best wavelet packet basis and corresponding transform coefficients can efficiently found from the fully quadtree decomposed result. With regard to a SAR image the procedures to find the best wavelet packet basis and the transform coefficient are as follows:

1. Fully decompose the initial image into frequency domain using quadtree decomposition.
2. Use the wavelet basis at the last scale as the best initial basis, and its cost as the best initial cost.
3. Trace back from the last scale, and comparing the cost at every node with the smallest cost in the all branches decomposed from the node. If the cost is reduced, update the best basis and the corresponding cost using this node; otherwise continue the backward search for the best basis.
4. The best basis and its transformed coefficients are found when the search comes toward the first scale, i.e., the initial spatial sampling data.

4. PROCESSING RESULTS

With the principles described, the clutter in a specific SAR image can be removed in the wavelet packet basis domain. The clutter removal is implemented by thresholding processing in the transform domain with a higher Signal-to-Clutter ratio compared with direct thresholding in spatial domain. But even the thresholding processing in transform domain will inevitably cause the target image loss, while the clutter is suppressed. In the processing, we choose a threshold level to keep

target image loss under an acceptable level, and allow some clutter residues to exist after the processing. The clutter residues can be easily removed by some post-processing such as additional thresholding and clustering processing in spatial domain. The processing scheme for SAR clutter reduction using AWPT method is shown in Figure 3. This clutter reduction scheme is applied to standard MSTAR SAR images [12]. A typical focused MSTAR image with clutters is shown in Figure 4. The image size is 128×128, and the resolution is about $0.3\,\mathrm{m} \times 0.3\,\mathrm{m}$. The target in the image is BTR-70 transportation vehicle, and the clutter was generated from background vegetation scattering. From the image, we can find that the reflections from the rear part of this vehicle are weak and indistinguishable from the background clutters due to the signal blockage by the front part of the target. It would be difficult to remove all clutters and keep the whole target signal intact using direct thresholding method.

4.1 Wavelet Filter for SAR Image Transform

Wavelet packet transform of an image can be implemented by recursive quad-tree decomposition of the original spatial sampling data. Based on "two-scale equations," the coefficients in the coarser scales can be derived from the coefficients in the finer scales. Considering the original sampling SAR data as the transform coefficients with the finest scale in spatial domain, we can obtain all wavelet packet transform coefficients by repeatedly filtering and down-sampling of the original spatial image using a wavelet filter. To maximally concentrate the energy of the transformed image, we choose Daubechies wavelet filter in this application. It is the most commonly used orthonormal wavelet filer; and the corresponding wavelet basis functions possess localization property in both time and frequency domains. The order of the wavelet filter is related to the vanishing moments of the wavelet basis functions. The higher the wavelet filter order, the more vanishing moments the basis functions, thus the more concentrated the transformed coefficients. However, through the convolution operation, the finest spatial resolution available for the transformed coefficients is the order of the wavelet filter. For a SAR image with scattering points in high spatial resolution, the wavelet filter of low order is desired for efficient representation of those scattering points in the transform domain. Therefore, we choose Daubechies filter with the order of 6 as the wavelet filters in this application. Using the AWPT algorithm based on

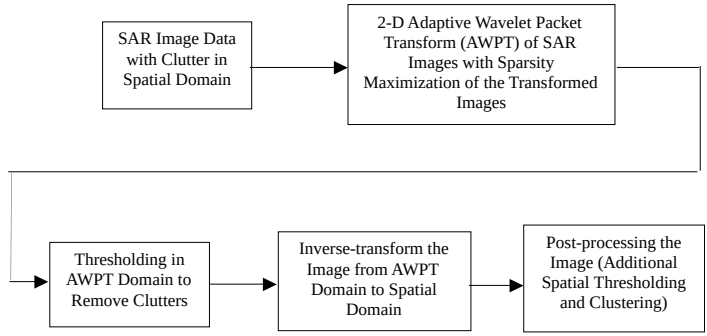

Figure 3. The processing scheme of automatic SAR clutter reduction based on Adaptive Wavelet Packet Transform (AWPT).

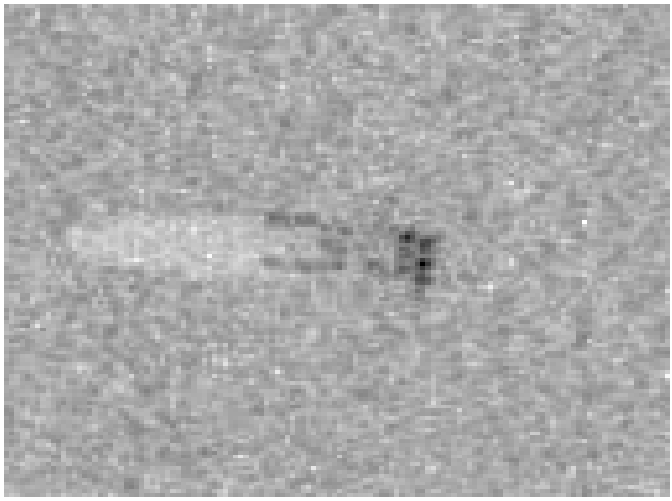

Figure 4. SAR image for BTR-70 transportation vehicle with vegetation clutters.

the quad-tree decomposition, we transformed BTR-70 image in Figure 4 into AWPT domain. The transformed image is displayed in Figure 5. The value of the corresponding energy concentration cost function is about 595 for the best wavelet packet basis, opposed to 777 of the cost function value in spatial domain; while the cost function value is about 641 if the conventional wavelet transform is applied to the image. Apparently we achieve the sparsest transformed image using the AWPT algorithm.

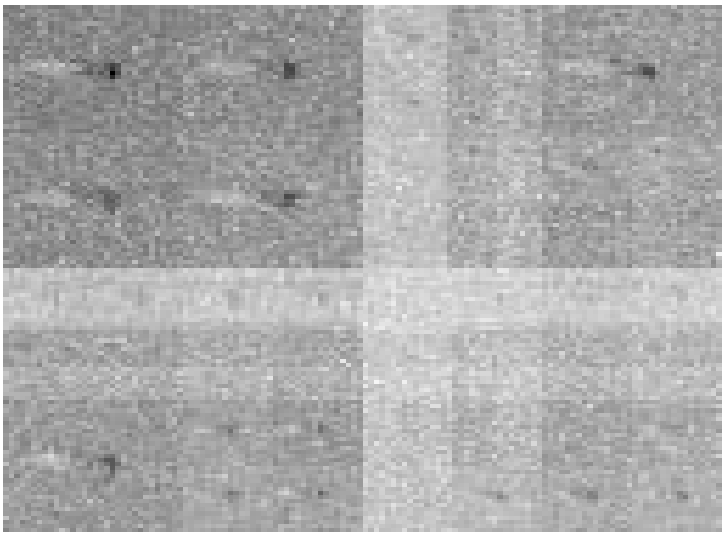

Figure 5. The basis transformed BTR-70 SAR image using AWPT.

4.2 Frequency-Dependent Thresholding

To remove clutters in the AWPT domain, we need to apply a threshold level to the transformed coefficients of SAR images. The common thresholding method is the soft-shrinkage proposed in [10], in which the above-threshold signal amplitude is reduced by a level of the threshold. The soft-thresholding is generally applicable to the cases that signals and noise or clutter are spatially overlapping. For SAR images, the target image and clutters are basically non-overlapping even in the transform domain. Hard-thresholding is a better choice, and it is defined as follows:

$$\hat{\widetilde{S}}(m,n) = \begin{cases} \widetilde{S}(m,n) & \text{if } \left|\widetilde{S}(m,n)\right| > T \\ 0 & \text{if } \left|\widetilde{S}(m,n)\right| \leq T \end{cases} \tag{27}$$

where: T is the threshold level.

If the spatial clutters are white and Gaussian distributed, the transformed clutters, as we have demonstrated, are still white and Gaussian distributed. Based on Newman-Pearson Criterion [15], the best threshold level is a constant provided that it meets requirements for

probabilities of false-alarm and target detection. But for SAR images, a pixel has some weak correlation with its adjacent pixels. Therefore, the clutter on a SAR image is not really white, and its power spectrum is stronger in lower frequencies. We design the threshold levels that are dependent on the central frequency for the quad-tree decomposition outputs at each of the final branches. For the output of one of outermost branches of the quad-tree decomposition, the central vertical and horizontal frequencies are assumed to be f_V and f_H, respectively, and the central frequency at that output branch is considered to be:

$$f_C = \sqrt{f_V^2 + f_H^2} \tag{28}$$

From quad-tree decomposition structure, we can find out the frequencies f_V and f_H, noting that due to the down-sampling, for two-channel decomposition of higher frequency band data, the high frequency components come out from low frequency filter output; while the low frequency components from high frequency filter outputs. Therefore the threshold level for the quad-tree decomposition output branch with central frequency f_C is:

$$T(f_C) = \frac{C \cdot \sigma_C}{\beta + f_C^{\alpha}} \tag{29}$$

where C is a constant, σ_c is the clutter standard deviation, and α and β are the parameters used to fit the mode to actual clutters. Therefore, the threshold level is the largest in low frequency, and the smallest in high frequency. Due to hard-thresholding processing, there is no DC energy loss for target image even with a high threshold level in near-DC areas. For MSTAR image processing we choose: $\alpha = 0.8 \sim 1$, and $\beta = 0$ in (29) to approximate the clutter spectrum characteristics and achieve the best clutter rejection performance. The AWPT transformed BTR-70 image is thresheld with parameters: $C = 0.5$, $\alpha = 0.85$, and $\beta = 0$ in (29), and shown in Figure 6. Using frequency-dependent threshold, we still can keep the delicate high-frequency components, which represent the important point-scattering reflections in the SAR images. But we could lose or blur the point-scattering signals after the processing if just using a constant threshold level for all transformed coefficients.

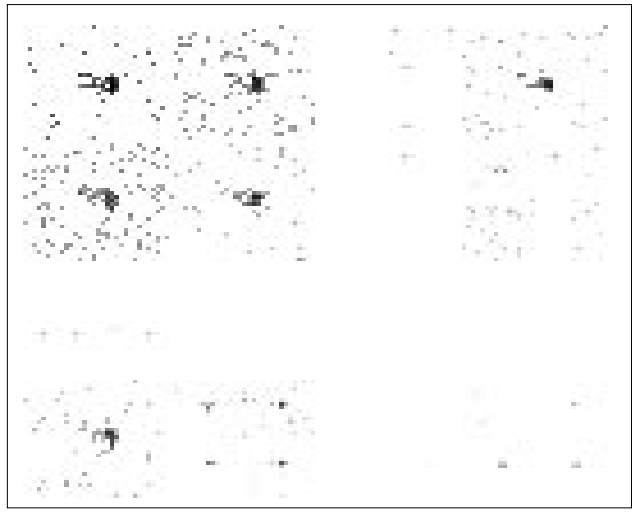

Figure 6. The transformed BTR-70 SAR image after frequency-dependent thresholding processing.

4.3 Post-Processing

Through thresholding processing most SAR image clutters are eliminated in the AWPT domain. The original SAR images can be restored by inverse-transforming the wavelet coefficients to spatial domain based on the same basis in the quad-tree decomposition. Similarly the inverse-transform can be efficiently implemented with filtering and up-sampling using another pair of filters $\{P(n)\}$ and $\{Q(n)\}$. Even with thresholding processing in AWPT, there are still some clutter residues existing. After the inverse-transform, those clutter resides will spread over SAR domain. Therefore, a second small threshold and a clustering processing are applied to the restored SAR image to further improve clutter rejection performance. The clustering algorithm replaces with zeros any connected non-zero blocks that have fewer elements than a pre-defined block size. Usually we set the block size to larger than the clutter residue sizes and smaller than target block size. For MSTAR images a clustering block size of 32 is usually enough to eliminate all clutter residues. Figure 7 is the restored BTR-70 image through post-processing with a second threshold level of about $0.1\sigma_c$. Also the best processing result using direct thresholding and clustering processing is shown in Figure 8. Apparently an essential part of the

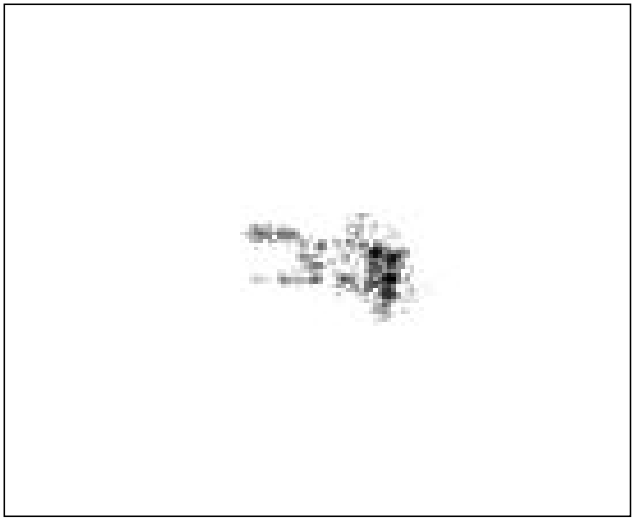

Figure 7. The restored BTR-70 image with thresholding in AWPT domain and post-processing in spatial domain.

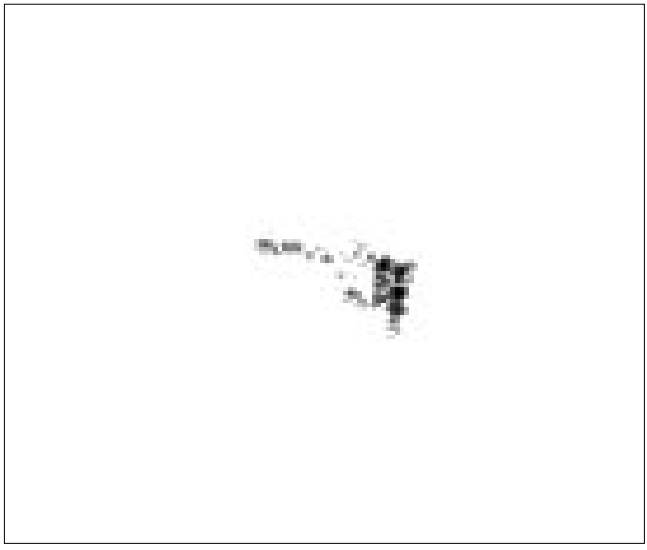

Figure 8. The de-cluttered BTR-70 image with direct thresholding processing in spatial domain.

target is lost in the direct thresholding processing because of low signal-to-clutter ratio in spatial domain, which thus poses a threat to correct target identification afterwards. Through the AWPT processing, the whole original target image is kept, while the clutters are completely removed.

4.4 Performance Metrics for MSTAR Data Processing

For a SAR image recovery processing the clutter rejection performance of an algorithm can be measured based on the ratio of mean square error to clutter standard deviation. But in the cases of absence of the original reference signals as for MSTAR images, the improvement of average target image signal-to-clutter ratio is a reasonable substitute. We define average target Signal-to-Clutter Ratio (SCR) as:

$$SCR = \frac{\sum_i \sum_j \left| \hat{S}(i,j) \right|}{N\sigma_C} \tag{30}$$

where $\hat{S}(i,j)$ is the processed target pixel, N is the total number of target image pixels, and σ_c is the clutter standard deviation.

The clutter rejection performance of an algorithm can be measured based on SCR improvements through its processing. In the AWPT clutter rejection processing, we gradually increase the AWPT domain threshold level, and measure the SCR improvements due to the thresholding processing in the AWPT domain (prior to the post-processing), while keeping the target image loss inside an acceptable range. Figure 9 shows SCR vs. the target image loss for three different kinds of MTSAR images through the AWPT processing. Target Image Loss (TIL) is defined as:

$$TIL = \frac{\overline{S} - \overline{\hat{S}}}{\overline{S}} \tag{31}$$

where $\overline{S}$ and $\overline{\hat{S}}$ are the average target signal amplitudes before and after the processing, respectively. For comparisons the SCR vs. TIL curves for Conventional Wavelet Transform (CWT) and direct thresholding are plotted in the same figures. We find that for a fixed target image loss, the AWPT algorithm almost always performs better than the CWT or direct thresholding method.

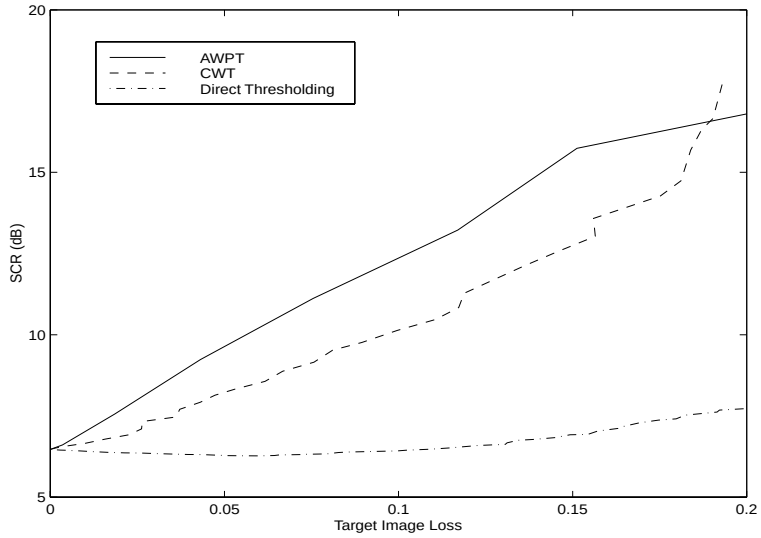

(a)

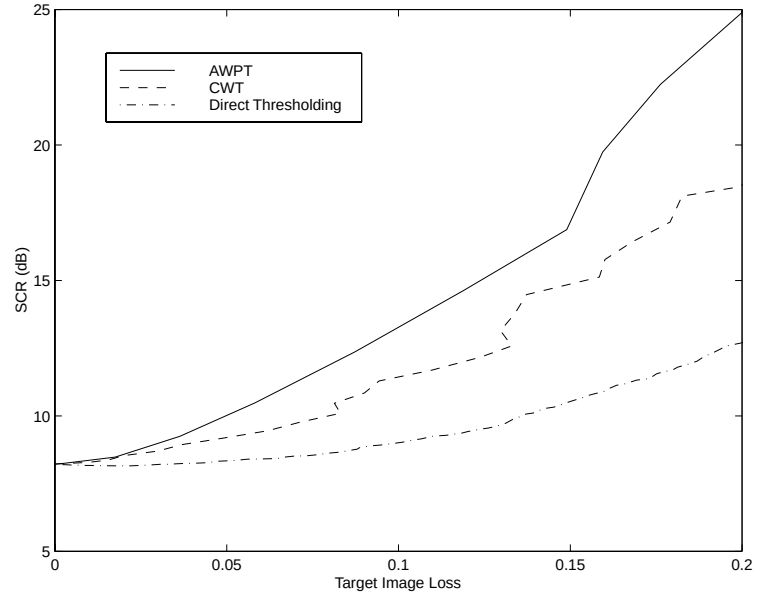

(b)

Figure 9. Signal-to-Clutter Ratio vs. target image loss using AWPT, CWT and direct thresholding methods for (a) BTR-70, (b) T-72.

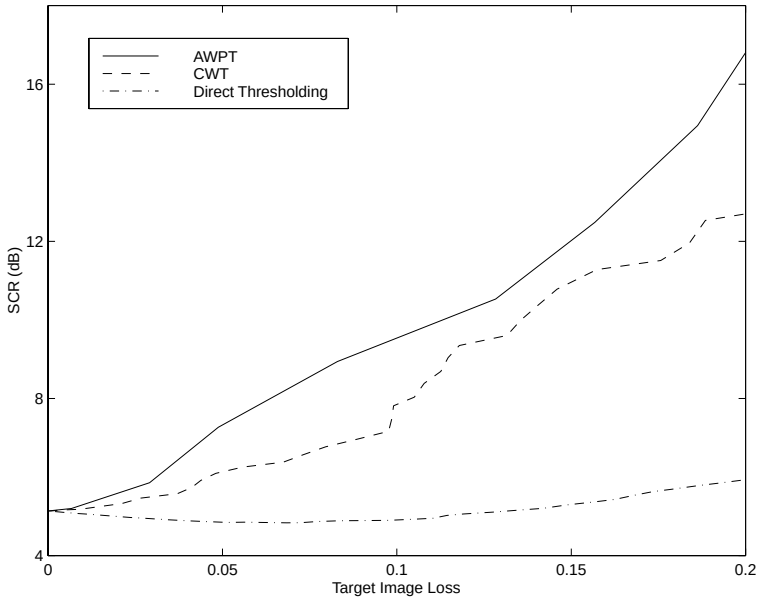

(c)

Figure 9. Signal-to-Clutter Ratio vs. target image loss using AWPT, CWT and direct thresholding methods for (c) BMP-2 targets.

5. CONCLUSIONS

We have developed a new clutter-rejection algorithm for SAR images based on Adaptive Wavelet Packet Transform (AWPT). It transforms the basis function of the SAR images from the regular pulse basis to a wavelet packet basis to make the transformed coefficients maximally concentrated on the transform domain. The transformed image has a higher target Signal-to-Clutter Ratio (SCR) compared with that in conventional spatial domain, thus the clutters can be removed in transform domain with less target signal losses. The method is based on the basic assumption that a clutter pixel in a SAR image is not or weakly correlated with one another; while target signals are strongly correlated to themselves. Thus, the SCR improvements are made possible through basis transformation.

The energy concentration function is used as the cost function to find the best wavelet packet basis to make the transformed coefficients

with the maximum SCR. The best basis search and the basis transformation for an image can be efficiently implemented using 2-D quad-tree decomposition algorithm. To search the best wavelet packet basis for a SAR image with clutters, it is very important to ensure either that the clutters and the target image are approximately non-overlapping after transformation in transform domain; or that the target energy is significantly stronger than the clutter one. Hence the best wavelet packet decomposition trees can be dominated by the target signals; otherwise the AWPT algorithm is not applicable.

A frequency-dependent thresholding method is introduced because the clutters in a SAR image are weakly correlated, i.e., they are "colored" rather than "white," as commonly assumed. The threshold level for the AWPT transformed outputs are chosen based on the central frequency of the data in this output. The lower the central frequency, the higher the threshold level. Simulation results show that the careless thresholding could degrade the performance of the AWPT algorithm to that of conventional wavelet transform, or even worse.

Processing results on MSTAR images show that this algorithm is very effective to remove the clutters for a SAR image with only limited clutter information such as standard deviation and rough spectrum characteristics required. With robust parameters pre-selected, the AWPT algorithm can be used to automatically remove the clutters in a large number of SAR images. But for the conventional direct thresholding method, it is usually very difficult to find a threshold level to remove all background clutters and keep the whole target image unaltered. This new method is also very useful for the situations in which the classical direct thresholding method might not work at all. Those situations include that some parts of target image signals are weaker than the clutter, or that the target signals and clutters are spatially over-lapping resulting from un-focused processing, or multi-path effects.

ACKNOWLEDGMENT

This work is supported by the Office of Naval Research under Contract No. N00014–98–1–0615.

REFERENCES

1. Wehner, D. R., *High Resolution Radar,* Artech, Norwood, MA, 1995.
2. Pham, D. H., A. Ezekel, M. T. Campbell, and M. J. T. Smith, "A new end-to-end SAR ATR system," *Proceedings of SPIE: Algorithms SAR Imagery VI,* Vol. 3721, 292–301, Orlando, Florida, April 1999.
3. Luo, D., *Pattern Recognition and Image Processing,* Horwood Publishing Limited, Chichester, England, 1998.
4. Wickerhauser, M. V., *Adapted Wavelet Analysis from Theory to Software,* A. K. Peters, Wellesley, Mass., 1994.
5. Chui, C. K., *An Introduction to Wavelets,* Academic Press, New York, 1992.
6. Daubechies, I., *Ten Lectures on Wavelets,* SIAM, Philadelphia, Penn., 1992.
7. Coifman, R. R., Y. Meyer, and M. V. Wickerhauser, "Wavelet analysis and signal processing," In *Wavelets and Their Applications,* 153–178, Jones and Barlett, Boston, 1992.
8. Mallat, S., *A Wavelet Tour of Signal Processing,* Academic Press, Inc., New York, 1998.
9. Deng, H. and H. Ling, "Fast solution of electromagnetic integral equations using adaptive wavelet packet transform," *IEEE Trans. Antennas Propagat.,* Vol. 47, 674–682, April 1999.
10. Donoho, D. L. and I. M. Johnstone, "Ideal spatial adaption by wavelet shrinkage," *Biometria,* Vol. 81, 425–455, Dec. 1994.
11. Odegard, J. E., H. Guo, M. Lang, C. S. Burrus, R. O. Wells, Jr., L. M. Novak, and M. Hiett, "Wavelet based SAR speckle reduction and image compression," Research Report, Comp. Math Lab., Rice Univ., and MIT Lincoln Lab., 1995.
12. *MSTAR SAR Data Set, Clutter and Targets,* collected by Sandia National Lab, released by DARPA, Apr. 1997.
13. Moulin, P., "A wavelet regularization method for diffuse radar-target imaging and speckle-noise reduction," *J. Math. Imag. and Vision,* No. 3, 123–134, 1993.
14. Irving, W. W., L. M. Novak, and A. S. Willsky, "A multiresolution approach to discrimination in SAR imagery," *IEEE Trans. Aerospace and Elec. Systems,* Vol. 33, No. 4, 1157–1168, Oct. 1997.
15. Skolnik, M. I., (Ed.), *Radar Handbook,* 2nd edition, McGraw-Hill, New York, 1990.
16. Van Trees, H. L., *Detection, Estimation, and Modulation Theory,* Part III, John Wiley & Sons, New York, 1971.

17. Papoulis, A., *Probability, Random Variables, and Stochastic Processes,* McGraw-Hill, New York, 1965.
18. Coifman, R. R. and M. V. Wickerhauser, "Entropy-based algorithms for best basis selection," *IEEE Trans. Info. Theory,* Vol. 38, 713–718, March 1992.
19. Donoho, D. L., "On minimum entropy segmentation," in *Wavelets: Theory, Algorithms, and Applications,* Academic Press, Inc., New York, 1994.